



Immobilization of $K_7PW_{11}O_{39}$ on ZrO_2 Nanofiber: Ultra-deep Desulfurization Based in Extraction Catalytic Oxidation Desulfurization System

GUOWEI ZENG, GUIHONG WU, ZHIHUI WANG, XIAONAN LI, JIE YANG, HONG ZHANG*

Institute of Polyoxometalate Chemistry, Department of Chemistry, Northeast Normal University, Changchun, Jilin 130024, PR China

Abstract: In this work, $K_7PW_{11}O_{39}$ (abbreviated as PW_{11}) was immobilized on ZrO_2 nanofibers and used as an efficient recyclable catalyst in extraction catalytic oxidation desulfurization system (ECODS). The 500 ppm DBT model oil (5 mL) can desulfurize completely within 20 min with the catalytic conditions of 50 °C, 0.010 g 50 wt% CTAB- PW_{11} - ZrO_2 nanofibers and O/S molar ratio (H_2O_2 /DBT molar ratio) was 2:1. The synthesized catalyst was characterized by Fourier transform infrared spectroscopy (FT-IR), powder X-ray diffraction (XRD), scanning electron microscope (SEM), transmission electron microscopy (TEM), energy dispersive spectroscopy (EDS) and thermo gravimetric analyzer (TGA). The results indicated the PW_{11} - ZrO_2 nanofibers were synthesized successfully and the possible catalytic mechanism is also revealed.

Keywords: desulfurization, polyoxometalate, nanofibres, ZrO_2 , PW_{11}

1. Introduction

The use of fuel is increasing year by year [1]. The combustion of organosulfur in fuel had already caused a series of environmental problems, such as the air pollution and the acid rain [2, 3]. Some countries introduced regulations to limit the sulfur content to below 10 ppm in fuel [4]. Ultra-deep desulfurization is in urgent demand.

Hydrodesulfurization (HDS) is a traditional technique for desulfurizing, which has been widely used in removing thiols, sulfides and disulfides. However, high cost, strict operation condition and long reaction time are main drawbacks of the HDS [1, 5]. Thus, several of other techniques emerged in recent years, such as oxidative desulfurization system (ODS) [6], adsorption [7] and bio-desulfurization [8-10]. Extraction catalytic oxidation desulfurization system (ECODS) has received extensive attention because of its excellent desulfurization efficiency under mild condition. So we conducted a series of explorations based on the ECODS.

The Keggin structure polyoxometallates (POMs) has applied to be the catalyst of the oxidation desulfurization, because it has unique properties and efficient catalytic performance. It was reported that monovalent Keggin-type phosphotungstate ($[PW_{11}O_{39}]^{7-}$) as heterogeneous catalysts in solvent-free ODS processes has an excellent catalytic performance [11]. However, pure POMs is hard to apply to industrial applications owing to high solubility and low surface area [12]. Therefore, our experimental work is mainly focus on improving its catalytic surface area and recycling capacity.

In our previous work, nanofiber materials performed well in the conversion of sulfide in ECODS [13, 14]. The surface of nanofibers has lots of loading sites and large specific surface area, which makes it easy to immobilize POMs. Besides, nanofibers can obtain easily via electrospinning [15]. ZrO_2 has been reported to enhance the removal reactivity of sulfides and the regeneration of catalysts with its acid resistance, high strength, large surface area and thermal chemical stability [16]. We also found that Zr-Based Metal-Organic Frameworks can accelerate the desulfurization process. So we immobilized PW_{11} on ZrO_2 nanofibers and synthesized a series of PW_{11} - ZrO_2 nanofibrous materials.

*email: hope20130122@163.com, zhangh@nenu.edu.cn, 2523414636@qq.com



Through the combination of ZrO_2 and PW_{11} , it may overcome the deficiency of high solubility and low surface area to suitable for industry scale desulfurization.

Herein, we explored the morphology, structure, optimal conditions of the desulfurization system, reusability and possible mechanism of PW_{11} - ZrO_2 nanofibers in this work. We found the PW_{11} - ZrO_2 nanofibers can desulfurize (5mL model oil contains 500 ppm DBT) completely in 20min with its optimal conditions: temperature is $50^\circ C$, H_2O_2 /DBT molar ratio is 2, the dosage of catalysts is 0.01g and the loading amount of PW_{11} on ZrO_2 is 50wt%. In addition, the catalyst can be reused over 6 times which prove immobilized PW_{11} on ZrO_2 nanofibers do increase the recycling capacity of PW_{11} .

2. Materials and methods

2.1 Chemicals

Zirconium(IV) butoxide solution (TNBZ, AR, Beijing Chemical Works), N,N-dimethylformamide (DMF, AR, Tianjin Tiantai Chemical Co. Ltd.), Ethanol (AR, Beijing Chemical Works), Polyvinyl pyrrolidone (PVP, MW = 1300000, Aladdin), Concentrated nitric acid (AR, Beijing Chemical Works), Cetyltrimethyl Ammonium Bromide (CTAB 99%, Energy Chemical), octadecyl trimethyl ammonium bromide (OTACl, 99%, Energy Chemical), dodecyl trimethyl ammonium bromide (DTACl, 99%, Energy Chemical), hydrogen peroxide (H_2O_2 , 30 wt%, Beijing Chemical Works), dibenzothiophene (DBT, 99%, China Pingmei Shenma Energy & Chemical Group Co., Ltd.), dichloromethane (AR, Tianjin Tiantai Chemical Co. Ltd.), n-octane, biphenyl (AR, Tianjin Tiantai Chemical Co. Ltd.), phosphotungstic acid (AR, Beijing Chemical Works), potassium chloride (AR, Beijing Chemical Works), sodium hydrogen phosphate dihydrate, sodium tungstate dihydrate (AR, Beijing Chemical Works), 1-Butyl-3-methylimidazolium hexafluorophosphate ([Bmim]PF₆, AR, Beijing Chemical Works). All chemicals are purchased directly without purification and treatment.

2.2 Synthesis and preparation of the materials

The synthesis process of ZrO_2 nanofibers: DMF (1.6 mL), absolute ethanol (1.6 mL), HNO_3 (1.0mL) and PVP (0.56g) added in a beaker. Stirring for half an hour. After that, TNBZ (0.52g) was added, and then the solution was stirred 30min to produce the spinning precursor. Then the obtained solution was put into a 5mL plastic syringe. We put one of electrode in the plastic syringe (immersed in solution), and then fix the other electrode on the iron net which 15.3cm away from the plastic syringe, electrospinning with a voltage of 15-16 kV. The droplets at the exit of the syringe are subjected to Coulombic and gravitational forces to form a continuous jet, which refines and stretches as the solvent volatilizes, and finally attaches to the receiver (iron net). After electrospinning, the ZrO_2 nanofibers were calcined at $600^\circ C$ to remove the PVP.

Immobilization of PW_{11} on ZrO_2 nanofibers: Potassium salts of $[PW_{11}O_{39}]^{7-}$ (PW_{11}) was synthesized according to the literature [17]. ZrO_2 nanofibers (0.060g) were dissolved in deionized water (10 mL) and ethanol (10 mL), stirring for 10h; PW_{11} (0.060g) and surfactants (0.060g) were dissolved in deionized water (10 mL) and ethanol (10 mL), stirring for 10h. Then mixing them and stirring for 24h. After that, washing the precipitations with water and ethanol. Ultimately, drying at $50^\circ C$ for 24h. The 50-CTAB- PW_{11} - ZrO_2 nanofibers were synthesized. A series of PW_{11} - ZrO_2 nanofibers prepared with similar way.

2.3 Desulfurization experiments

DBT (0.1g) and biphenyl (0.2g, as the standard substance) dissolved in n-octane(100mL), and the model oil with sulfur content of 500ppm was prepared. Then, putting model oil (5mL), IL ([Bmim]PF₆), H_2O_2 (definitive amount) and catalysts (definitive amount) into a flask. The upper oil sample was analyzed on gas chromatography (Agilent 7820A) after reacting for a while.

2.4 Characteristics

The infrared (FT-IR) absorption spectra were examined with KBr Pelles on a Mattson Alpha-Centauri Fourier transform infrared spectrometer, and the range was fixed in $4000\text{--}400\text{ cm}^{-1}$ with the number of scan 64 and the resolution 4 cm^{-1} . Thermogravimetric analysis (TG) was implemented on a Perkin-Elmer Thermal Analyzer under nitrogen atmosphere at a heating rate of $10^\circ\text{C}/\text{min}$. XRD analysis used a Powder Rigaku D/max-RA XRD which 2θ range from 10° to 80° with Cu $K\alpha$ radiation. Transmission electron microscope (TEM) analysis was carried out using a JEM-2010 transmission electron microscope. The elemental analysis and mapping of product were employed using OXFORD ISIS-300 energy-dispersive spectrometer. The Agilent 7820A-GC System using DB-5 chromatographic column with $30\text{m}\times 0.32\text{mm}\times 0.25\mu\text{m}$ was used to GC analysis, and injection port temperature was 200°C , detector temperature was 250°C , and 150°C was immobilized as oven temperature.

3. Results and discussions

3.1 Catalysts characterization

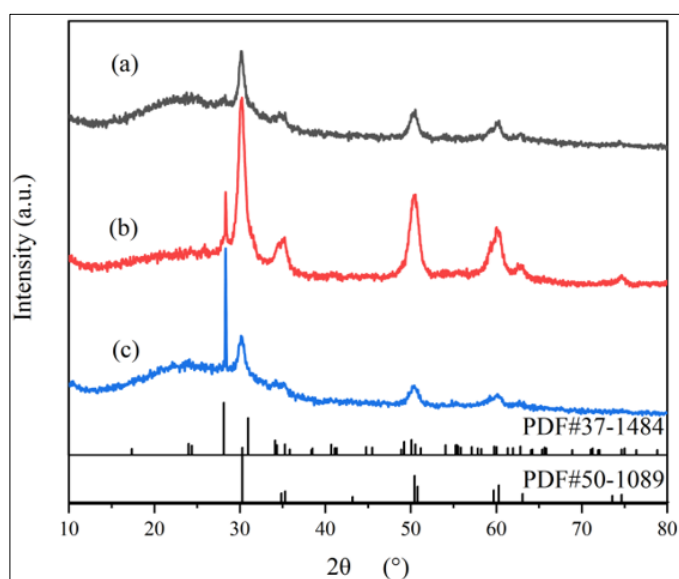


Figure 1. PXRD spectra of 50-CTAB-PW₁₁-ZrO₂ nanofibers(a), 50-DTA-PW₁₁-ZrO₂ nanofibers(b) and 50-OTA-PW₁₁-ZrO₂ nanofibers(c)

We used PXRD analysis (2θ , $10^\circ\text{--}80^\circ$) to research the structure of 50-CTAB-PW₁₁-ZrO₂ nanofibers. Figure S1 showed the PXRD spectra of 50-CTAB-PW₁₁-ZrO₂ nanofibers and 50-CTAB-PW₁₁-ZrO₂ nanofibers after six cycles which are pure t-phase ZrO₂ (PDF#50-1089). It proves that the structure of the catalyst is unchanged after six cycles. We also explored the phase structure of PW₁₁-ZrO₂ materials with various cations. From Figure 1, 50-DTA-PW₁₁-ZrO₂ nanofibers and 50-OTA-PW₁₁-ZrO₂ nanofibers appeared the characteristic peaks of mixture t-phase (PDF#50-1089) and monoclinic phase ZrO₂ (PDF#37-1484), implying the structure of the ZrO₂ will change with different cations.

Figure 2 displayed the FT-IR spectra of 50-CTAB-PW₂-ZrO₂ (a), PW₁₁ (b) and CTAB (c), the peaks in $2700\text{--}3000\text{ cm}^{-1}$ are considered to be the characteristic bands of C–H stretching modes for carbon chain. So the bands of 2916 and 2843 cm^{-1} are contributed by CTA⁺ from Figure 2c. Figure 2b showed characteristic peaks of P–O, W=O and W–O–W stretch located at 1094 and $1040/948$; 879 and 784 cm^{-1} , respectively [18–20]. The 50-CTAB-PW₁₁-ZrO₂ had characteristic peaks of both PW₁₁ and CTAB.

We find the characteristic peaks of PW₁₁ in Figure 2a are changed to $957, 902$ and 712 cm^{-1} ; it's maybe due to the strong interaction between PW₁₁ and CTAB [21]. In addition, the Figure S2 showed FT-IR spectra of different loading amounts.

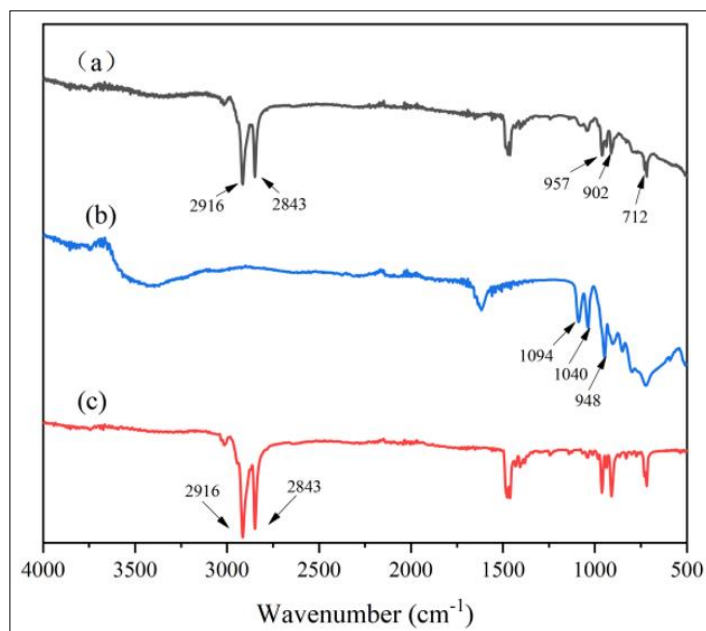


Figure 2. FT-IR spectra of 50-CTAB-PW₁₁-ZrO₂ (a), PW₁₁ (b) and CTAB (c)

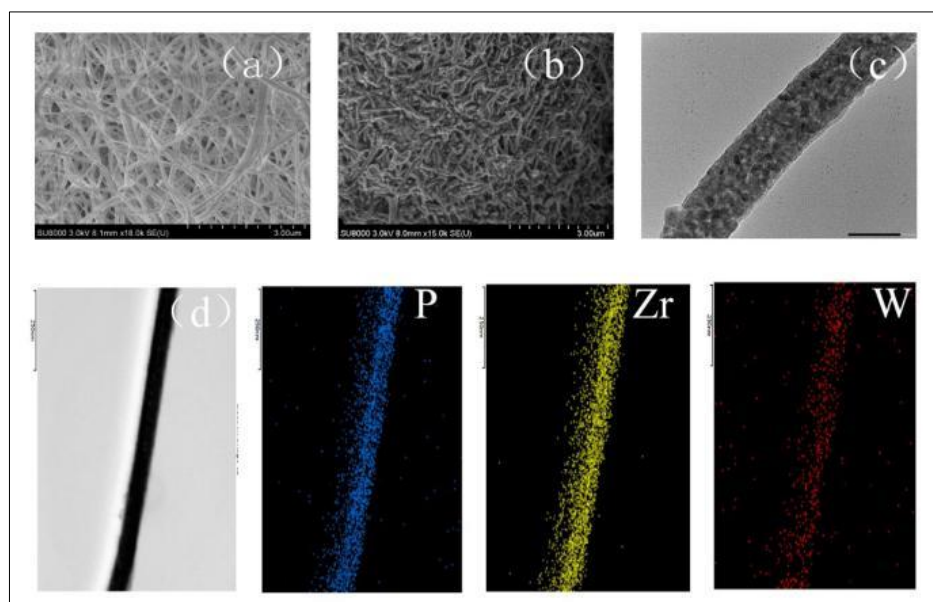


Figure 3. SEM images of 50-CTAB-PW₁₁-ZrO₂ nanofibers (a) and 50-CTAB-PW₁₁-ZrO₂ after six cycles (b), TEM image of CTAB-11 -ZrO₂ nanofibers (c), elemental mapping (d)

FE-SEM showed the surface morphologies of 50-CTAB-PW₁₁-ZrO₂ and 50-CTAB-PW₁₁-ZrO₂ after six cycles. In Figure 3a, fibrous ZrO₂ evenly distributed on the image, which showed uniform diameters. After cycling, these fibers gathered together due to agitation during the reaction (Figure 3b), which may reduce the catalytic efficiency. From Figure 3c, many obvious black spots were prominent on the ZrO₂ nanofibers [22]. It proved that PW₁₁ are loaded on the nanofibers. As the elemental mapping showed in Figure 3(d), P, W, Zr had excellent dispersibility on the ZrO₂ nanofibers. It also illustrated these elements are present in the catalyst. The energy dispersive spectrum (EDS) was also investigated. Zr, O, W, C, N and P elements were observed in Figure 4 and Figure 5. The results proved that 50-CTAB-PW₁₁-ZrO₂ nanofiber was highly pure and the element of the catalyst is unchanged after six cycles.

In addition, we treated the catalyst at high temperature, the thermogravimetric (TG) image showed that the catalyst remains stable in mass below 100°C (Figure S3).

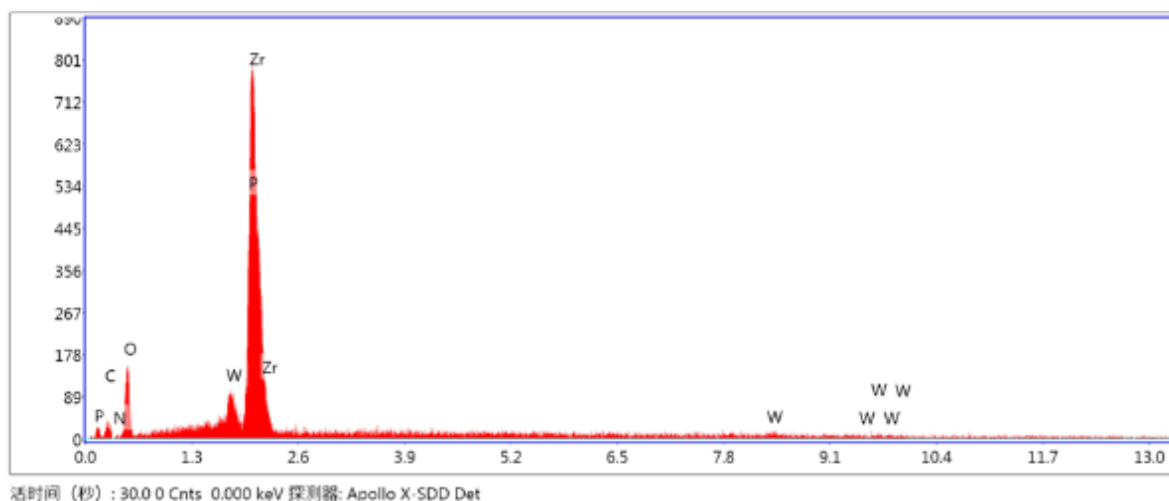


Figure 4. EDS of 50-CTAB-PW₁₁-ZrO₂ nanofibers

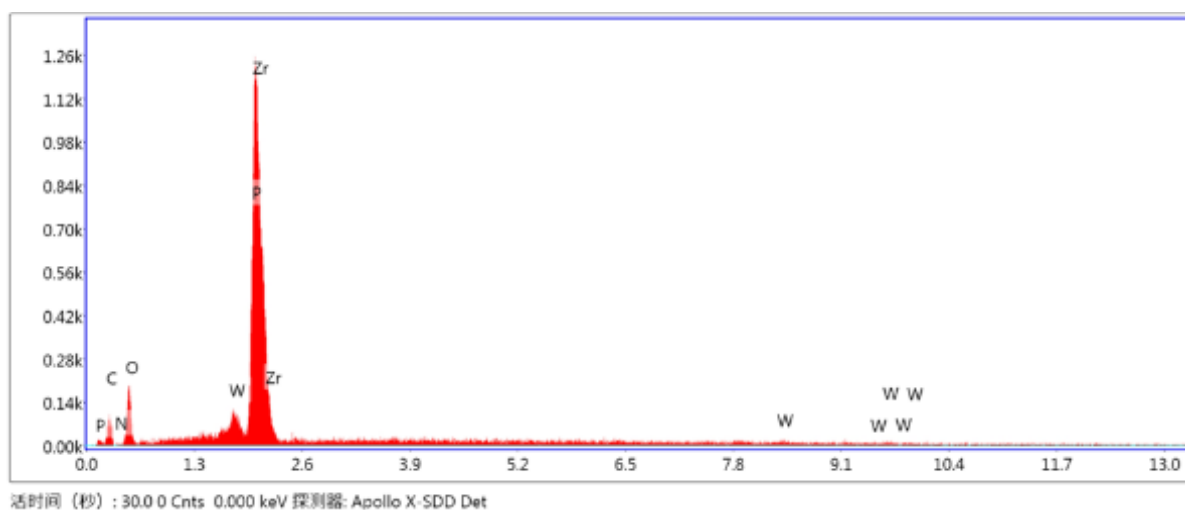


Figure 5. EDS of 50-CTAB-PW₁₁-ZrO₂ nanofibers after six cycles

3.2 Catalytic performances

3.2.1 The impact of Different systems and different catalysts

Figure 6 exhibits desulfurization efficiency of 50-CTAB-PW₁₁-ZrO₂ nanofibers, POMs and bare ZrO₂ nanofibers. The PW₁₁ showed a high catalytic activity, which removed sulfur completely under 60min. But the desulfurization efficiency is still lower than the 50-CTAB-PW₁₁-ZrO₂ nanofibers. A possible reason is PW₁₁ has the water solubility. DBT removal efficiency is 7.2% for bare ZrO₂ nanofibers in 60min; it may be due to the physical adsorptive capacity of bare ZrO₂ nanofibers. However, when PW₁₁ loaded on the ZrO₂ nanofibers, the desulfurization time reduced to 20min. It proved that there is an interaction between PW₁₁ and ZrO₂ nanofibers in the 50-CTAB-PW₁₁-ZrO₂ nanofibers to improve the catalytic performance.

We compared the desulfurization efficiency with different PW₁₁ catalysts in Table S1. We found that CTAB-PW₁₁-ZrO₂ nanofibers have better catalytic performance than other catalysts.

3.2.2 The impact of temperature on desulfurization

As the main factor of oxidative desulfurization efficiency, reaction temperature on DBT conversion is investigated (Figure 7). With the reaction temperature of 30°C, the sulfur removal time are 40min. when the temperature increasing to 50 and 70°C, the required time for complete sulfur removal was reached in 20 min. The reason for the different DBT conventional speed is related to the acceleration of molecular motion. Higher temperature will accelerate the movement of molecules [23, 24]. However, high temperature can also cause the self-decomposition of H₂O₂, resulting in the reduction of efficiency [25]. Considering the economizing energy and reaction efficiency, 50°C are chosen as an optimal temperature.

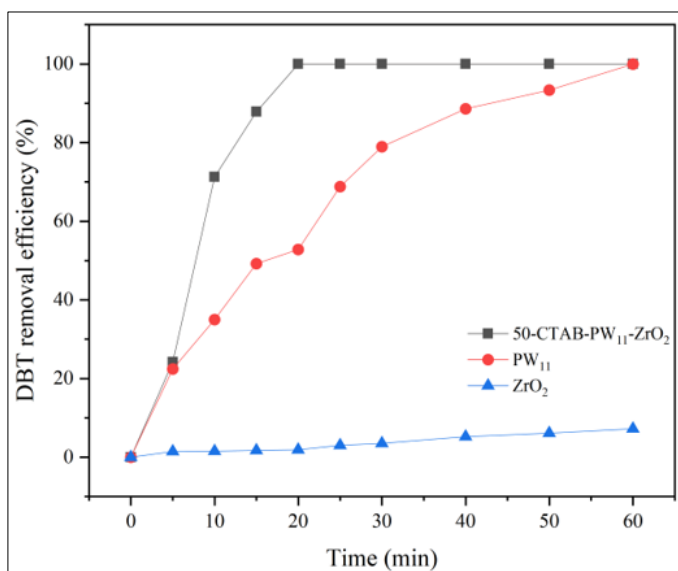


Figure 6. Desulfurization efficiency of 50-CTAB-PW₁₁-ZrO₂ nanofibers, PW₁₁ and bare ZrO₂ nanofibers. Reaction conditions: 50°C, O/S = 2, mcat = 0.01g, 50-CTAB-PW₁₁-ZrO₂ nanofibers

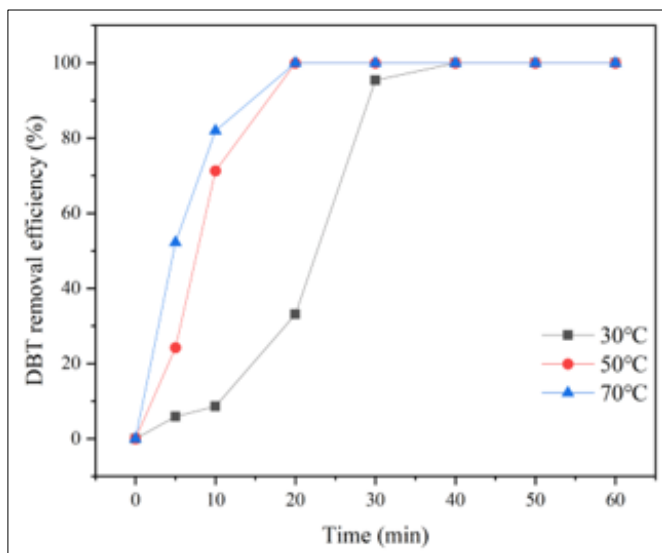


Figure 7. Influences of different temperature. Reaction conditions: O/S = 2, mcat = 0.01g, 50-CTAB-PW₁₁-ZrO₂ nanofibers

3.2.3 Desulfurization efficiency of different H₂O₂/DBT (O/S) molar ratio

The amount of oxidant also profoundly affects the catalytic efficiency. In terms of stoichiometric relationship, 1 mol H₂O₂ can oxidize 2 mol sulfone [26]. We chose a series of different proportions of O/S molar ratio (1:1, 2:1, 4:1 and 8:1) to test the DBT removal efficiency. In Figure 8, the best O/S molar ratio is 2:1. When the ratio of O/S molar ratio increases to 4:1 and 8:1, the DBT removal time extends to 30 and 60min. The reduction of catalyst efficiency is due to the nonproductive decomposition of H₂O₂ itself, and more oxidants will increase the rate of self-decomposition [27], which means more

water will be led into this reaction system. That will cause a decrease in the concentration of active sites [28]. Therefore, the 2:1 is the most appropriate O/S molar ratio.

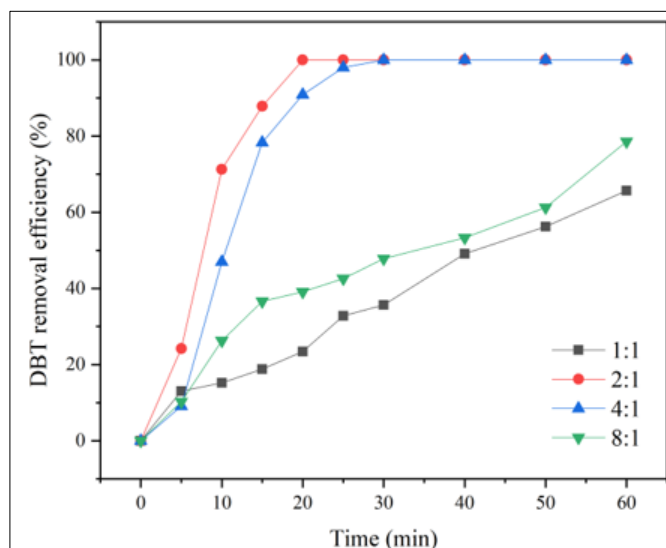


Figure 8. Influences of different O/S molar ratio. Reaction conditions: 50°C, mcat = 0.01 g, 50-CTAB-PW₁₁-ZrO₂ nanofibers

3.2.4 Influence of different cations on DBT removal

We compared the desulfurization efficiency with different cations. As could be observed in Figure 9, the 50-CTAB-PW₁₁-ZrO₂ nanofibers used 20min to remove the DBT altogether, while the 50-DTA-PW₁₁-ZrO₂ nanofibers and 50-OTA-PW₁₁-ZrO₂ nanofibers taking 25min to achieve 100% desulfurization efficiency. The length of the carbon chain will affect the catalytic efficiency [29]. Long single-alkyl chain will provide a dual trap for both DBT and H₂O₂, but it's not conducive to the contact between sulfide and the active site of catalyst when the single-alkyl chain is too long [30]. So the CTAB was chosen as the suitable cation.

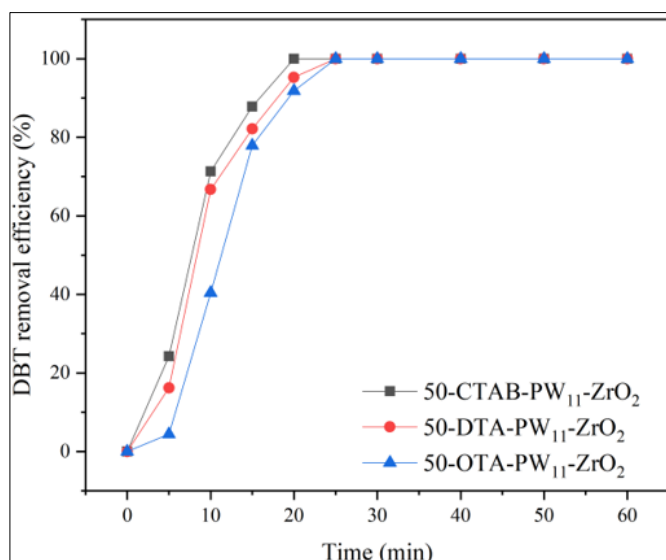


Figure 9. Influences of different cations. Reaction conditions: 50°C, O/S = 2, mcat = 0.01 g

3.2.5 The impact of 50-CTBA-PW11 nanofibers dosage on desulfurization efficiency

Figure 10 showed the impact of catalyst dosage. The DBT was removed within 40 and 20min by using 0.005 and 0.010g catalyst, respectively. When the catalyst dosage increased to 0.020g, it also used 20min to complete desulfurization. The aggregation of nanofibers may have occurred, because of the excess catalysts. Accordingly, we concluded the best dosage of 50-CTAB-PW₁₁-ZrO₂ nanofibers was 0.01g.

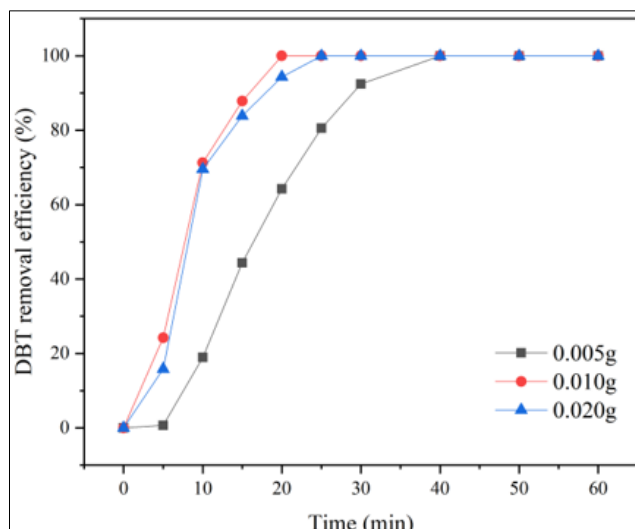


Figure 10. Influences of 50-CTAB-PW₁₁-ZrO₂ nanofibers dosage. Reaction conditions: 50°C, O/S= 2, 50-CTAB-PW₁₁-ZrO₂ nanofibers

3.2.6 The effect of CTAB-PW₁₁-ZrO₂ nanofibers loading amount on DBT removal

The CTAB-PW₁₁-ZrO₂ nanofibers loading amount is a leading role for desulfurization, which determines the number of active species. Figure 11 shows the desulfurization efficiency of different CTAB-PW₁₁-ZrO₂ nanofibers loading amount. It took about 20 and 30 min with 50wt% and 60wt% of CTAB-PW₁₁-ZrO₂ nanofibers loading amount to remove sulfur completely. The probable cause was the excess catalysts cover of active sites [31]. Therefore we chose 50wt% as the best loading amount for the sake of saving catalyst.

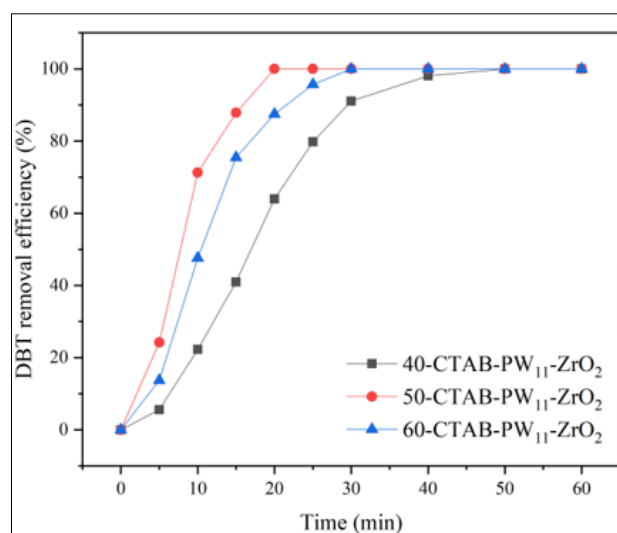


Figure 11. Influences of CTAB- PW₁₁-ZrO₂ Nanofibers loading amount. Reaction conditions: 50°C, O/S = 2, mcat = 0.01 g

3.2.7 Recycling

After each reaction was completed, the catalyst was collected by centrifugation and washed with methylene dichloride. When 50-CTAB-PW₁₁-ZrO₂ nanofibers was put in the oven for 8h (80°C) and dried again, it was collected for desulfurization experiments. As shown in Figure 12, 50-CTAB-PW₁₁-ZrO₂ nanofibers could maintain high DBT catalytic efficiency (higher than 95%), after going through six cycles. The results revealed that 50-CTAB-PW₁₁-ZrO₂ nanofibers could recycle at least six times.

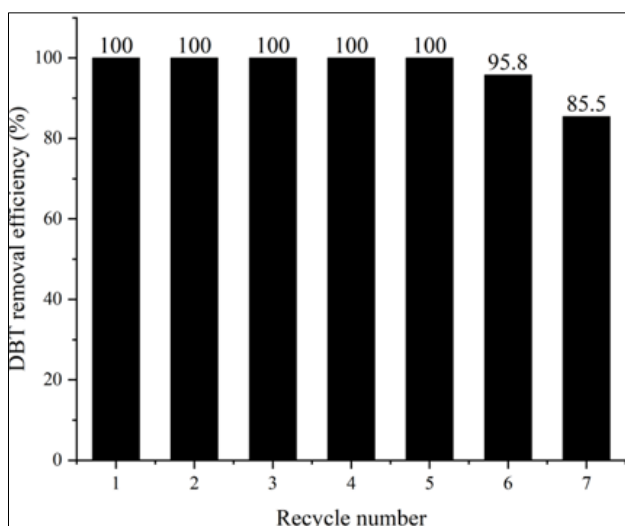


Figure 12. Recycle performance of 50-CTAB-PW₁₁-ZrO₂ nanofibers. Reaction conditions: 50°C, O/S = 2, mcat = 0.01 g, 50-CTAB-PW₁₁-ZrO₂ nanofibers

3.2.8 Mechanism

Figure 13 illustrated the ECODS mechanism of CTAB-PW₁₁-ZrO₂ nanofiber. There are three phases in this system: oil phase (containing DBT), H₂O₂ phase (containing oxidative agent) and IL phase (dispersive catalysts). Magnetic stirring makes the three phases in fully contact. H₂O₂ will approach PW₁₁ [32], because of its hydrophily. DBT will tend to the carbon chain, because of its hydrophobicity. At the beginning of the catalytic process, [Bmim]PF₆ extracted DBT to IL phase, and then W=O of PW₁₁ was oxidized to peroxo species W (O₂). After that, the peroxo species W (O₂) oxidised DBT to DBTO₂ while peroxo species W (O₂) reducing into W=O [33]. DBTO₂ has a high polarity, so it will remain at IL phase, resulting in a sustained decrease of DBT concentration in oil.

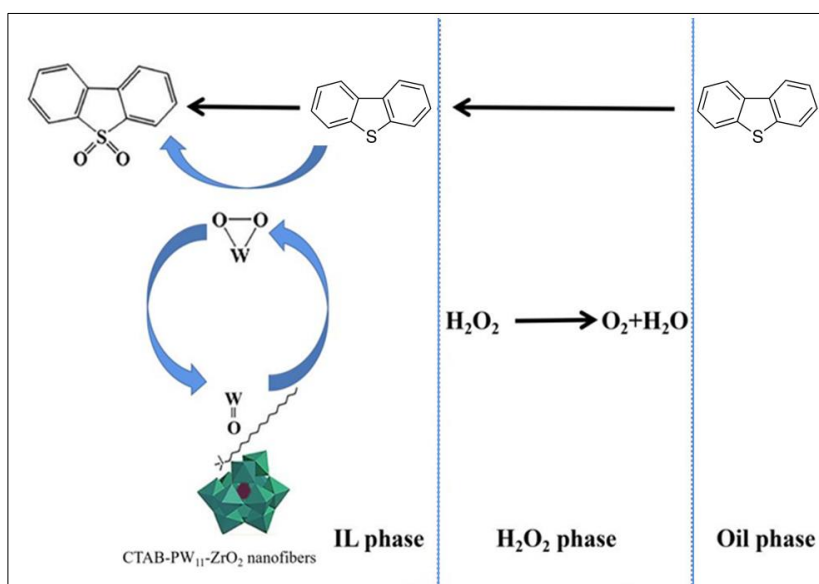


Figure 13. Proposed desulfurization mechanism of 50-CTAB-PW₁₁-ZrO₂ nanofibers

4. Conclusions

In this work, catalyst for desulfurization were successfully synthesized by electrospinning and applied to the desulfurization process. The DBT could be removed completely within 20 min with catalytic conditions of 50°C, 0.010g 50-CTAB-PW₁₁-ZrO₂ nanofibers and ratio of O/S molar was 2:1. It showed the excellent catalytic effect of PW₁₁ immobilized on ZrO₂ nanofibers. Besides, the catalyst could be easily reused for six consecutive cycles.



Acknowledgements. We gratefully acknowledge financial support from the National Natural Science Foundation of China (21571032 and 21271038) and the Analysis and Testing Foundation of Northeast Normal University.

References

- 1.L. BAN, P. LIU, C. MA, B. DAI, Deep oxidative/adsorptive desulfurization of model diesel oil by DBD/FeCl₃-SiO₂, *Catalysis Today*, 211, 2013, 78-83.
- 2.R. ZHAO, J. WANG, D. ZHANG, Y. SUN, B. HAN, N. TANG, N. WANG, K. LI, Biomimetic oxidative desulfurization of fuel oil in ionic liquids catalyzed by Fe (III) porphyrins, *Applied Catalysis A: General*, 532, 2017, 26-31.
- 3.E. ESEVA, A. AKOPYAN, A. SCHEPINA, A. ANISIMOV, A. MAXIMOV, Deep aerobic oxidative desulfurization of model fuel by Anderson-type polyoxometalate catalysts, *Catalysis Communications*, 149, 2021, 106256.
- 4.A. STANISLAUS, A. MARAFI, M. S. RANA, Recent advances in the science and technology of ultra low sulfur diesel (ULSD) production, *Catalysis Today*, 153, 2010, 1-68.
- 5.Y. GAO, Z. LV, R. GAO, G. ZHANG, Y. ZHENG, J. ZHAO, Oxidative desulfurization process of model fuel under molecular oxygen by polyoxometalate loaded in hybrid material CNTs@MOF-199 as catalyst, *J Hazard Mater*, 359, 2018, 258-265.
- 6.A. W. BHUTTO, R. ABRO, S. GAO, T. ABBAS, X. CHEN, G. YU, Oxidative desulfurization of fuel oils using ionic liquids: A review, *Journal of the Taiwan Institute of Chemical Engineers*, 62, 2016, 84-97.
- 7.J. BU, G. LOH, C. G. GWIE, S. DEWIYANTI, M. TASRIF, A. BORGNA, Desulfurization of diesel fuels by selective adsorption on activated carbons: Competitive adsorption of polycyclic aromatic sulfur heterocycles and polycyclic aromatic hydrocarbons, *Chemical Engineering Journal*, 166, 2011, 207-217.
- 8.P. A. ÇELİK, D. Ö. AKSOY, S. KOCA, H. KOCA, A. ÇABUK, The approach of biodesulfurization for clean coal technologies: a review, *International Journal of Environmental Science and Technology*, 16, 2019, 2115-2132.
- 9.S. RANGRA, M. KABRA, V. GUPTA, P. SRIVASTAVA, Improved conversion of Dibenzothiophene into sulfone by surface display of Dibenzothiophene monooxygenase (DszC) in recombinant *Escherichia coli*, *J Biotechnol*, 287, 2018, 59-67.
- 10.S. M. PAIXAO, B. F. AREZ, J. C. ROSEIRO, L. ALVES, Simultaneously saccharification and fermentation approach as a tool for enhanced fossil fuels biodesulfurization, *J Environ Manage*, 182, 2016, 397-405.
- 11.F. MIRANTE, B. DE CASTRO, M. G. C., S. B. S, Solvent-Free Desulfurization System to Produce Low-Sulfur Diesel Using Hybrid Monovacant Keggin-Type Catalyst, *Molecules*, 25, 2020.
- 12.M. A. REZVANI, Z. SHOKRI AGHBOLAGH, H. HOSSEINI MONFARED, S. KHANDAN, Mono Mn(II)-substituted phosphotungstate@modified graphene oxide as a high-performance nanocatalyst for oxidative demercaptanization of gasoline, *Journal of Industrial and Engineering Chemistry*, 52, 2017, 42-50.
- 13.A. JUNKAEW, P. MAITARAD, R. ARRÓYAVE, N. KUNGWAN, D. ZHANG, L. SHI, S. NAMUANGRUK, The complete reaction mechanism of H₂S desulfurization on an anatase TiO₂ (001) surface: a density functional theory investigation, *Catalysis Science & Technology*, 7, 2017, 356-365.
- 14.J. FU, Y. GUO, W. MA, C. FU, L. LI, H. WANG, H. ZHANG, Syntheses and ultra-deep desulfurization performance of sandwich-type polyoxometalate-based TiO₂ nanofibres, *Journal of Materials Science*, 53, 2018, 15418-15429.
- 15.P. C. HSU, S. WANG, H. WU, V. K. NARASIMHAN, Y. CUI, Performance enhancement of metal nanowire transparent conducting electrodes by mesoscale metal wires, *Nature Communications*, 4, 2013, 2522.



16. E. Sasaoka, N. Sada, A. Manabe, M. A. U Dd In and Y. Sakata, Modification of ZnO-TiO₂ high-temperature desulfurization sorbent by ZrO₂ addition, *Industrial & Engineering Chemistry Research*, **38**, 1999, 958-963.
17. S. AOKI, T. KURASHINA, Y. KASAHARA, T. NISHIJIMA, K. NOMIYA, Polyoxometalate (POM)-based, multi-functional, inorganic-organic, hybrid compounds: syntheses and molecular structures of silanol- and/or siloxane bond-containing species grafted on mono- and tri-lacunary Keggin POMs, *Dalton Trans*, 40, 2011, 1243-1253.
18. G. F. TOURNÉ, C. M. TOURNÉ, *Progress in Polytungstophosphate and -arsenate(V) Chemistry*, 1994.
19. J. Iijima, H. Naruke, Structural characterization of Keggin sandwich-type [LnIII(α -PW₁₁O₃₉)₂]₁₁ (Ln = La and Ce) anion containing a pseudo-cubic LnIII O₈ center, *Inorganica Chimica Acta*, 379, 2011, 95-99.
20. S. RIBEIRO, C. M. GRANADEIRO, P. SILVA, F. A. ALMEIDA PAZ, F. F. DE BIANI, L. CUNHA-SILVA, S. S. BALULA, An efficient oxidative desulfurization process using terbium-polyoxometalate@MIL-101(Cr), *Catalysis Science & Technology*, 3, 2013, 2404.
21. K. LI, X. YANG, Y. GUO, F. MA, H. LI, L. CHEN, Y. GUO, Design of mesostructured H₃PW₁₂O₄₀-titania materials with controllable structural orderings and pore geometries and their simulated sunlight photocatalytic activity towards diethyl phthalate degradation, *Applied Catalysis B Environmental*, 99, 2010, 364-375.
22. N. LIU, X. WANG, W. XU, H. HU, J. LIANG, J. QIU, Microwave-assisted synthesis of MoS₂/graphene nanocomposites for efficient hydrodesulfurization, *Fuel*, 119, 2014, 163-169.
23. Z. Lv, R. Gao, G. Zhang, Y. Zheng and J. Zhao], Oxidative desulfurization process of model fuel under molecular oxygen by polyoxometalate loaded in hybrid material CNTs@MOF-199 as catalyst, *Journal of Hazardous Materials*, 2018.
24. Y. GAO, R. GAO, G. ZHANG, Y. ZHENG, J. ZHAO, Oxidative desulfurization of model fuel in the presence of molecular oxygen over polyoxometalate based catalysts supported on carbon nanotubes, *Fuel*, 224, 2018, 261-270.
25. Y. DING, W. ZHU, H. LI, W. JIANG, M. ZHANG, Y. DUAN, Y. CHANG, Catalytic oxidative desulfurization with a hexatungstate/aqueous H₂O₂/ionic liquid emulsion system, *Green Chemistry*, 13, 2011, 1210-1216.
26. H. LÜ, S. WANG, C. DENG, W. REN, B. GUO, Oxidative desulfurization of model diesel via dual activation by a protic ionic liquid, *Journal of Hazardous Materials*, 279, 2014, 220-225.
27. R. NOYORI, M. AOKI, K. SATO, Green oxidation with aqueous hydrogen peroxide, *CHEMICAL COMMUNICATIONS- ROYAL SOCIETY OF CHEMISTRY*, 2003.
28. Z. Jian, B. Aw, A. Yw, A. Hw and A. Jg, Heterogeneous oxidative desulfurization of diesel oil by hydrogen peroxide: Catalysis of an amphiphatic hybrid material supported on SiO₂ - ScienceDirect, *Chemical Engineering Journal*, **245**, 2014, 65-70.
29. A. NISAR, J. ZHUANG, X. WANG, Construction of amphiphilic polyoxometalate mesostructures as a highly efficient desulfurization catalyst, *Advanced Materials*, 23, 2011, 1130-1135.
30. H. LI, X. JIANG, W. ZHU, J. LU, Y. YAN, Deep Oxidative Desulfurization of Fuel Oils Catalyzed by Decatungstates in the Ionic Liquid of [Bmim]PF₆, *Industrial & Engineering Chemistry Research*, 48, 2009, 9034-9039.
31. C. KOMINTARACHAT, W. TRAKARNPRUK, Oxidative Desulfurization Using Polyoxometalates, *Industrial & Engineering Chemistry Research*, 45, 2006, págs. 1853-1856.
32. KAIWEN, ZHANG, HONG, YAN, WENWEN, Electrospinning synthesis of H₃PW₁₂O₄₀/TiO₂ nanofiber catalytic materials and their application in ultra-deep desulfurization, *Applied Catalysis A General an International Journal Devoted to Catalytic Science & Its Applications*, 526, 2016, 147-154.
33. S. O. RIBEIRO, D. JULIAO, L. CUNHA-SILVA, V. F. DOMINGUES, R. VALENCA, J. C. RIBEIRO, B. DE CASTRO, S. S. BALULA, Catalytic oxidative/extractive desulfurization of model and untreated diesel using hybrid based zinc-substituted polyoxometalates, *Fuel*, 166, 2016, 268-275.

34.F. MIRANTE, L. DIAS, M. SILVA, S. O. RIBEIRO, M. C. CORVO, B. DE CASTROA, C. M. GRANADEIROA, S. S. BALULAA, Efficient heterogeneous polyoxometalate-hybrid catalysts for the oxidative desulfurization of fuels, *Catalysis Communications*, 2018, S156673671730417X.

35.N. WU, B. LI, Z. LIU, C. HAN, Synthesis of Keggin-type lacunary 11-tungstophosphates encapsulated into mesoporous silica pillared in clay interlayer galleries and their catalytic performance in oxidative desulfurization, *Catalysis Communications*, 46, 2014, 156-160.

36.Z. E. A. ABDALLA, B. LI, Preparation of MCM-41 supported $(\text{Bu}_4\text{N})_4\text{H}_3(\text{PW}_{11}\text{O}_{39})$ catalyst and its performance in oxidative desulfurization, *Chemical Engineering Journal*, 200-202, 2012, 113-121.

37.ZAKI, ELDIN, ALI, ABDALLA, BAOSHAN, LI, ASMA, TUFAIL, Direct synthesis of mesoporous $(\text{C}_{19}\text{H}_{42}\text{N})_4\text{H}_3(\text{PW}_{11}\text{O}_{39})/\text{SiO}_2$ and its catalytic performance in oxidative desulfurization, *Colloids & Surfaces A Physicochemical & Engineering Aspects*, 2009

Manuscript received: 02.02.2021

Electronic Supporting Information (ESI)

1.XRD patterns of CTAB-PW₁₁-ZrO₂ nanofibers and CTAB-PW₁₁-ZrO₂ nanofibers after six cycles.

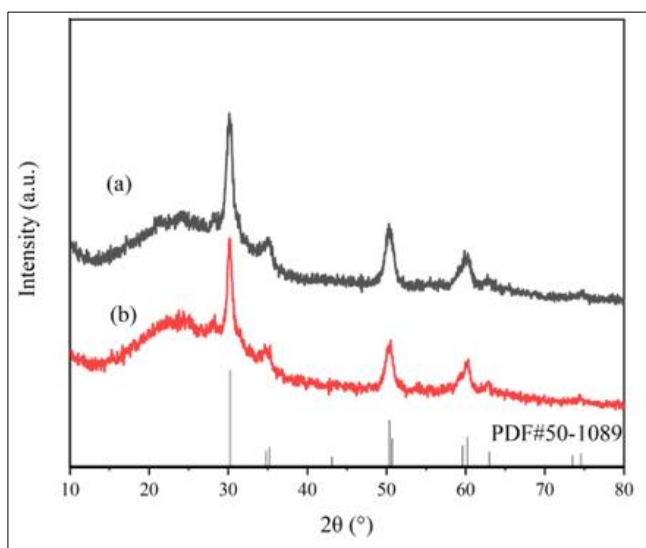


Figure S1 XRD patterns of CTAB-PW₁₁-ZrO₂ nanofibers(a) and CTAB-PW₁₁-ZrO₂ nanofibers after six cycles(b)

Figure S1 showed the PXRD spectra of CTAB-PW₁₁-ZrO₂ nanofibers and CTAB-PW₁₁-ZrO₂ nanofibers after six cycles. It indicates the CTAB-PW₁₁-ZrO₂ nanofibers and catalyst after circulation are pure t-phase ZrO₂(PDF#50-1089), which has diffraction peaks of 30.270, 35.255, 50.377, 59.610, 60.205. It proves that the structure of the catalyst is unchanged after six cycles

2.FT-IR spectra of different loading amounts.

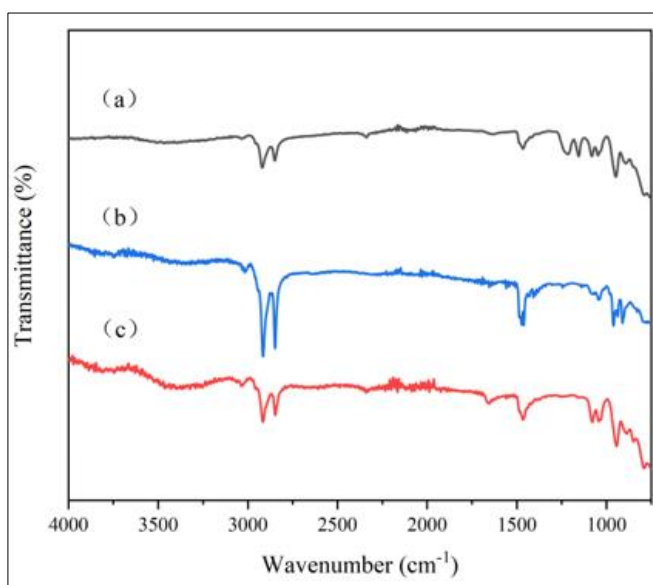


Figure S2 FT-IR spectra of 40% wt-CTAB-PW₁₁-ZrO₂ (a), 50% wt-CTAB-PW₁₁-ZrO₂ (b), 60% wt-CTAB-PW₁₁-ZrO₂(c)

Figure S2 showed 40% wt-CTAB-PW₁₁-ZrO₂(a), 50% wt-CTAB-PW₁₁-ZrO₂(b) and 60% wt-CTAB-PW₁₁-ZrO₂(c) have similar spectra. This means the intact structure of catalysts still retain under different loading amount

3. Thermogravimetric (TG) image of CTAB-PW₁₁-ZrO₂ nanofibers.

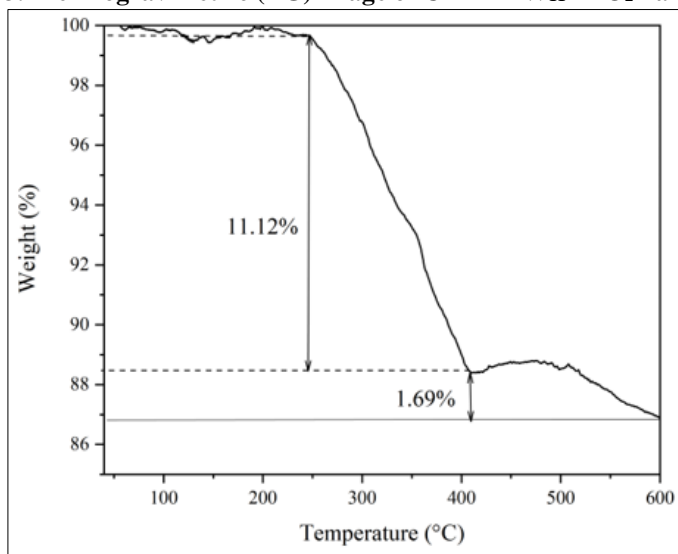


Figure S3 TG image of CTAB-PW₁₁-ZrO₂ nanofibers

Figure S3 showed that the catalyst remains stable in mass below 100°C, which proved PW₁₁-ZrO₂ nanofibers can function as a desulfation catalyst under mild conditions

4. Table for DBT removal efficiency of different catalysts

Entry	Catalysts	t/min	T/°C	Desulfurization efficiency (%)	Ref.
1	Tb (PW ₁₁) 2 @ MIL-101	120min	50	100	1[20]
2	ODAPW ₁₁	40min	70	100	2[34]
3	PW ₁₁ / MSPM	120min	60	99.7	3[35]
4	PW ₁₁ / MCM-41	60min	70	99.82	4[36]
5	PW ₁₁ / SiO ₂	90min	60	99.96	5[37]
6	CTAB-PW ₁₁ -ZrO ₂ NF	20min	50	100	This work